

---

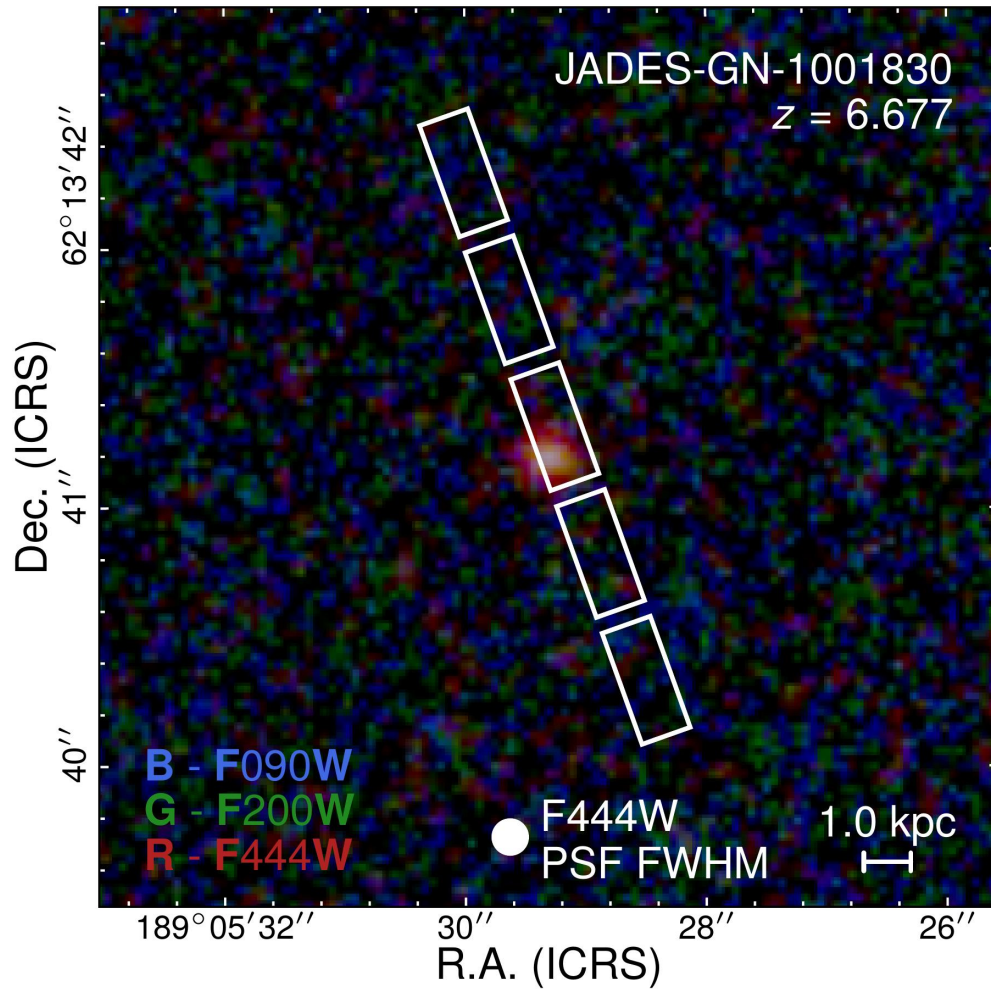
**Supplementary information**

---

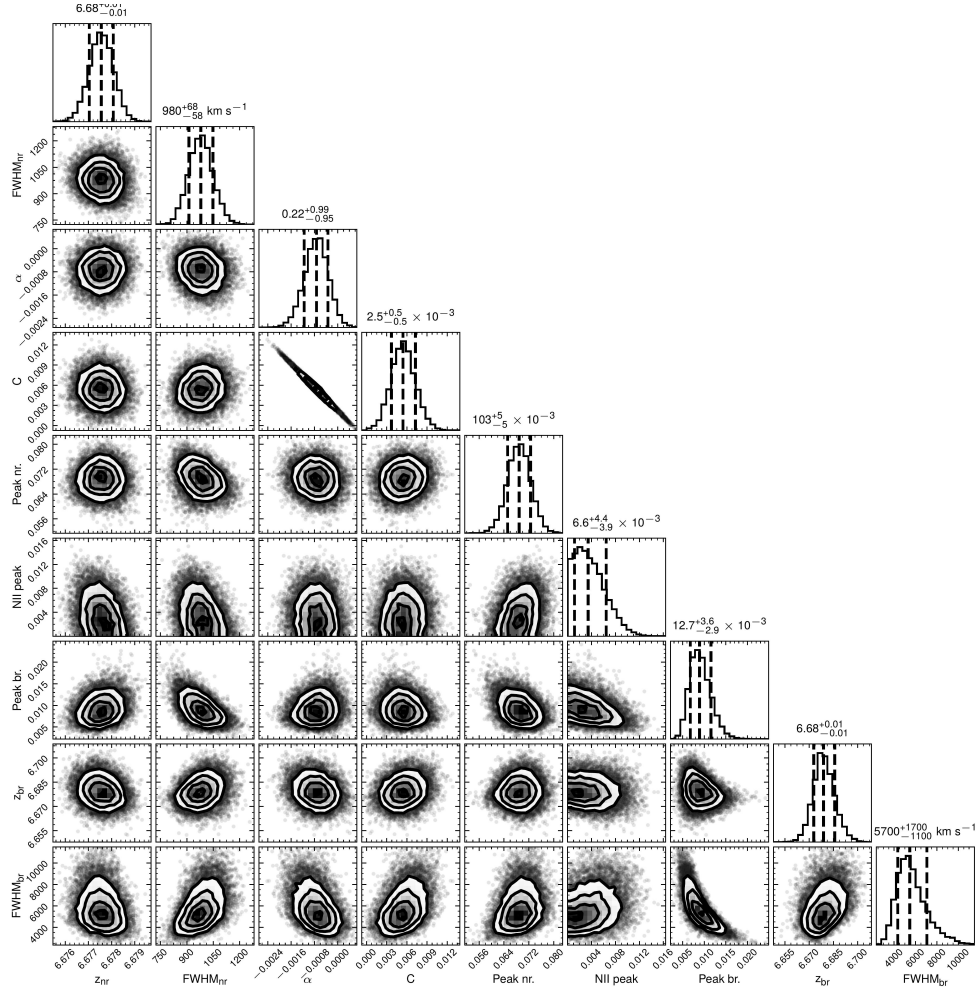
**A dormant overmassive black hole in the early Universe**

---

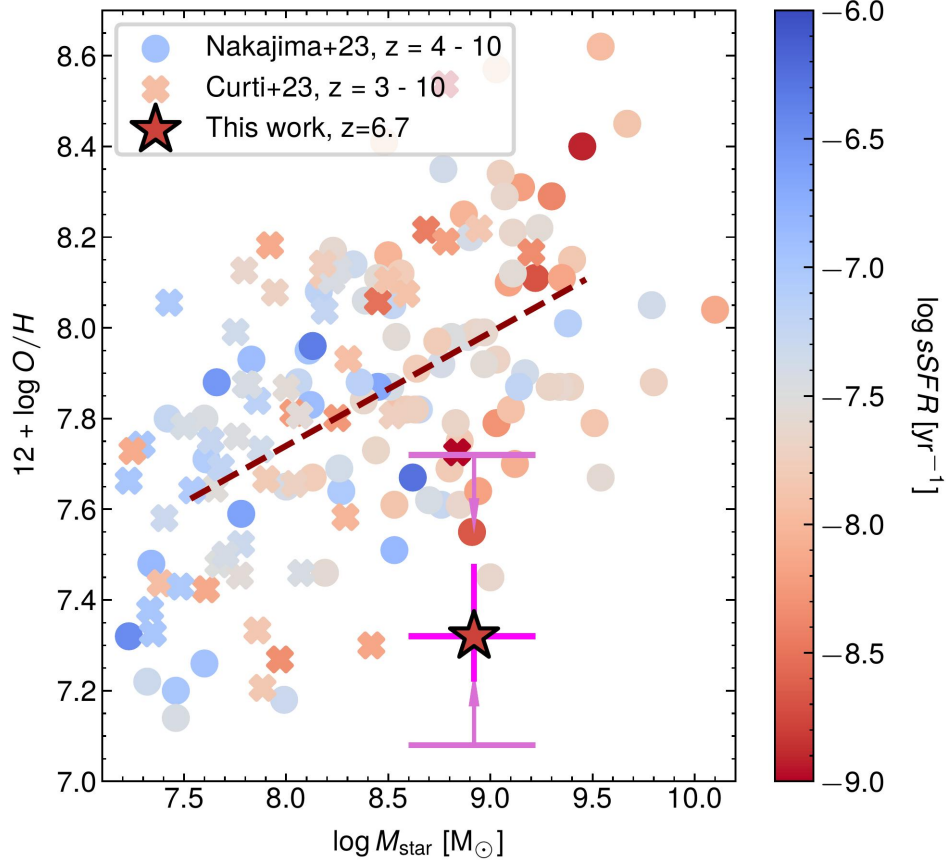
In the format provided by the authors and unedited



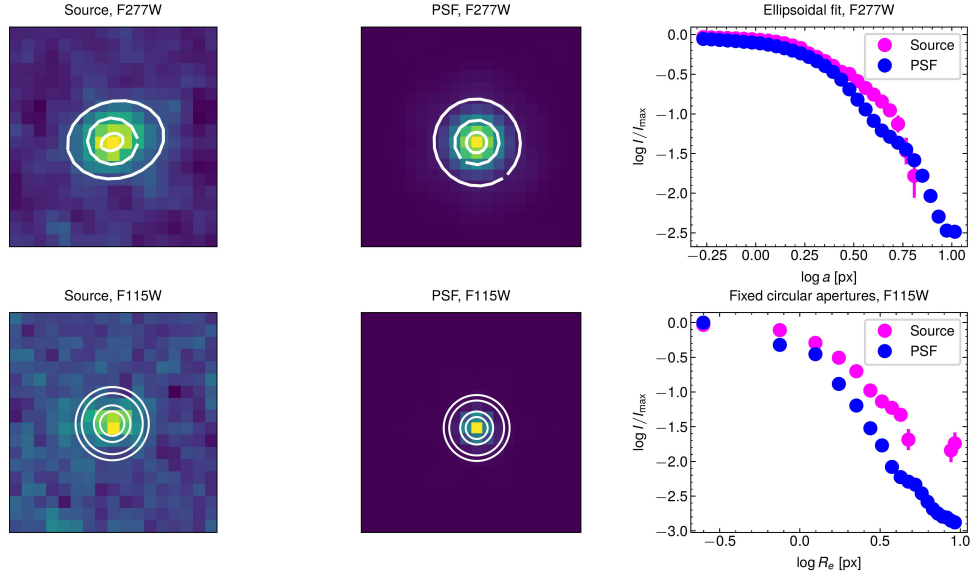
**Supplementary Material Fig. 1: Image of GN-1001830.** A red-green-blue (RGB) image of the AGN and galaxy in the F444W, F277W and F115W bands. A 1 kpc physical scale bar is overplotted alongside the FWHM of the PSF in the F444W band. The position of the NIRSpect slit is also overplotted.



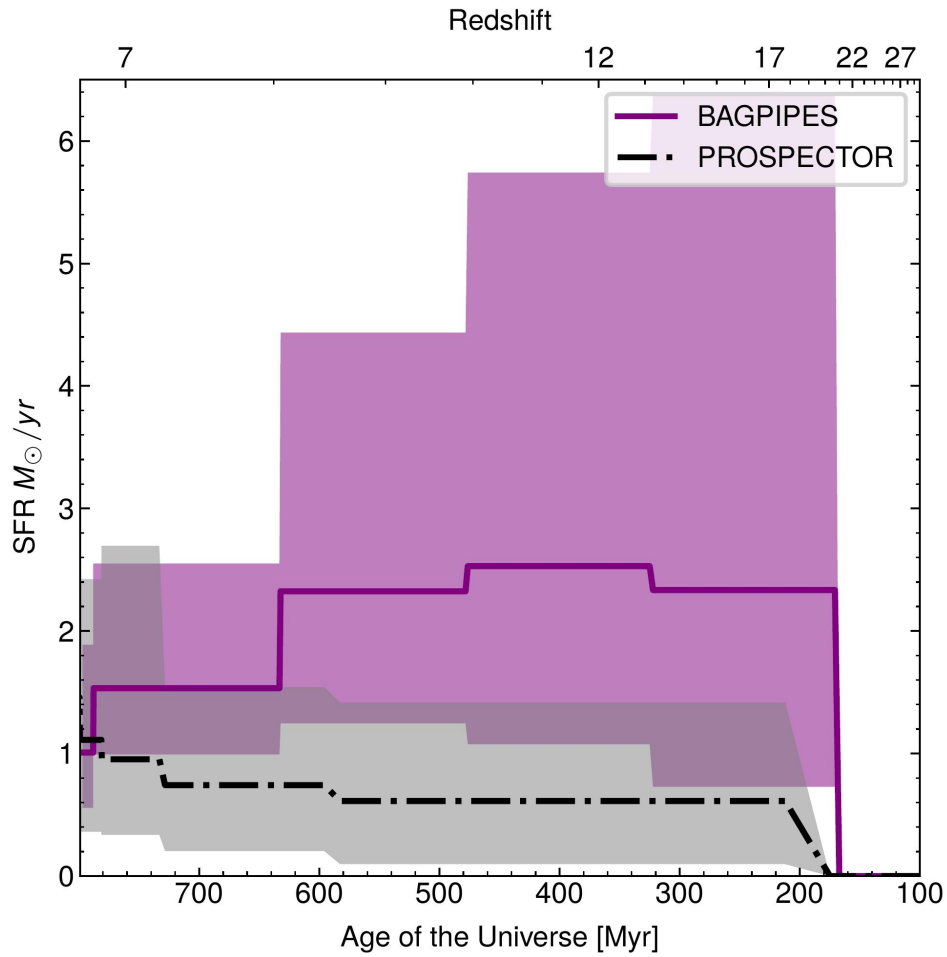
**Supplementary Material Fig. 2: A corner plot summarizing the MCMC fit results of the H $\alpha$  profile.** Here  $\alpha$  and  $C$  are the continuum slope and normalization respectively, "Peak nr." and "Peak br." show the peak heights of the narrow and broad H $\alpha$  components respectively. The FWHM values given are not corrected for instrumental broadening. The total spectrum was normalized to unity before fitting, hence peak heights are unitless here. The [S II] doublet parameters are not shown as it is undetected.



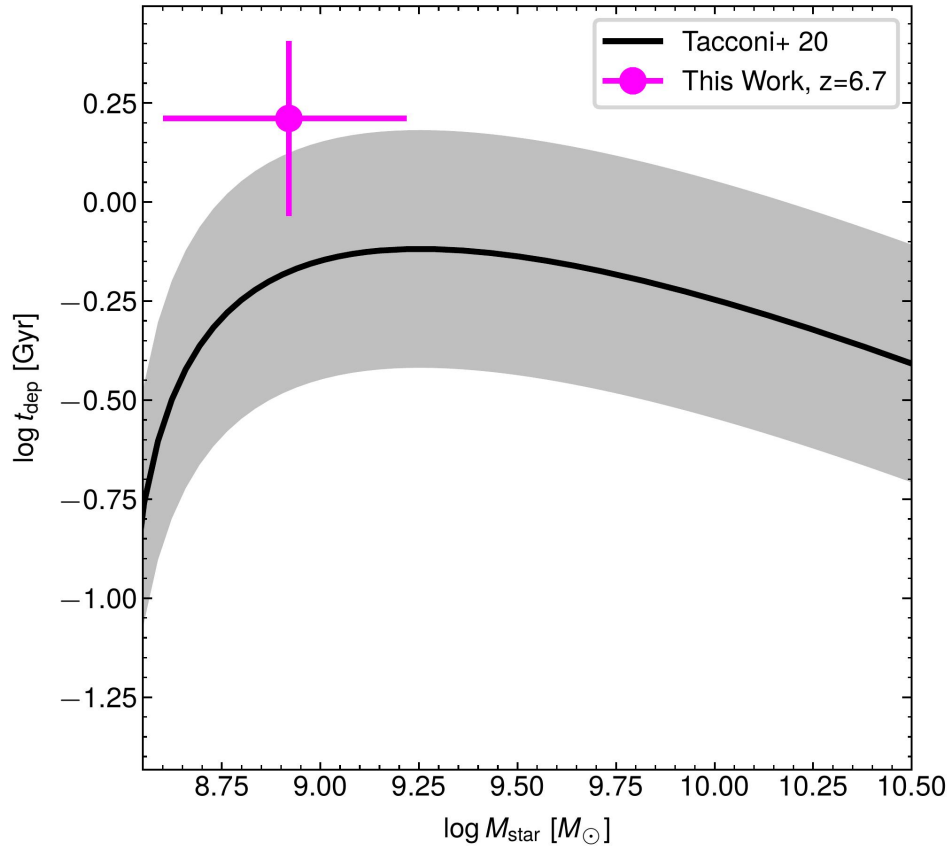
**Supplementary Material Fig. 3: Mass-metallicity relation** Location of GN-1001830 (large star with magenta errorbars) relative to the mass-metallicity relation at  $z = 4 - 10$  obtained by [1] and [2] (circles and crosses) whose best fit is shown with the brown dashed line. The lighter colored magenta bars show the upper and lower limits for the metallicity of GN-1001830. All markers are colored according to their specific star formation rate,  $\log(sSFR)$ .



**Supplementary Material Fig. 4: Radial profile diagrams.** Comparisons of our object images with the model PSFs in the F277W (top row) and F277W (bottom row) bands. The top row shows the radial profiles for both source (magenta) and PSF (blue) obtained by fitting elliptical isophotes (shown in white in the cutouts). The bottom row shows the radial profiles in F115W band given by measuring fluxes in concentric circular apertures. All radial profiles measured are normalized to the maximum intensity and presented in log-scale. Both methods also reveal GN-1001830 to have a significant extended component.



**Supplementary Material Fig. 5: SFH comparisons.** A comparison between the SFHs given by the two different codes used. While both SFHs are quite uncertain, they consistently show that the galaxy experienced a roughly constant SFR between 1 and 2  $M_{\odot} \text{ yr}^{-1}$  for most of its lifetime.



**Supplementary Material Fig. 6: Depletion time.** Location of GN-1001830 (magenta point) with respect to the depletion time versus stellar mass scaling relation for sources with the same SFR taken from [3] (solid black line). The grey shading represents the  $\sim 0.3$  dex intrinsic scatter on the relation.

## References

- [1] Nakajima, K. *et al.* JWST Census for the Mass-Metallicity Star Formation Relations at  $z = 4-10$  with Self-consistent Flux Calibration and Proper Metallicity Calibrators. *ApJS* **269** (2), 33 (2023). <https://doi.org/10.3847/1538-4365/acd556>, [arXiv:2301.12825](https://arxiv.org/abs/2301.12825) [astro-ph.GA].
- [2] Curti, M. *et al.* JADES: Insights into the low-mass end of the mass-metallicity-SFR relation at  $3 < z < 10$  from deep JWST/NIRSpec spectroscopy. *A&A* **684**, A75 (2024). <https://doi.org/10.1051/0004-6361/202346698>, [arXiv:2304.08516](https://arxiv.org/abs/2304.08516) [astro-ph.GA].
- [3] Tacconi, L. J., Genzel, R. & Sternberg, A. The Evolution of the Star-Forming Interstellar Medium Across Cosmic Time. *ARA&A* **58**, 157–203 (2020). <https://doi.org/10.1146/annurev-astro-082812-141034>, [arXiv:2003.06245](https://arxiv.org/abs/2003.06245) [astro-ph.GA].